University of Zawia Journal of Engineering Sciences and Technology (UZJEST)
Volume 2, Issue 1, (2024), pp 81-97, ISSN 3006-2764

Simulation of Laminar Nanofluids Flow over a Heated Double Backward-Facing Step

Ali K. A. Alriqeeq[1*], Shaban A. A. Jolgam[2]

[1]Mechanical Engineering Department, Faculty of Engineering, Sabratha University, Sabratha, Libya.
[2]Mechanical Engineering Department, Faculty of Engineering, University of Zawia, Zawia, Libya.

*Corresponding author email: alialriqeeq12@gmail.com

Received: 31-05-2024 | Accepted: 13-06-2024 | Available online: 15.06.2024 | DOI:10.26629/uzjest.2024.08

ABSTRACT

This research focuses on heat transfer enhancement by separating flow over a double backward-facing step using nanofluid. To conduct this research, a numerical model was constructed using the ANSYS Workbench, and the governing equations were solved using the realizable *k*-ε model with a second-order upwind scheme. Three different types of base fluid (water, engine oil, and ethylene glycol) with nanoparticles (AL_2O_3, TiO_2, and Cu) were used for Reynolds numbers ranging from 200 to 1000. The constant heat flux of the 2000 W/m^2 boundary condition is considered on the lower wall. The effect of nanoparticle material, nanoparticle concentrations, nanoparticle sizes, and Reynolds numbers on the Nusselt number is investigated. Two different approaches for estimating nanofluid thermal conductivity and viscosity have been used. The numerical code results were verified with previous numerical data. The results showed that the peak of the Nusselt number occurs immediately after the steps. The results demonstrated a significant improvement in the heat transfer performance of nanofluids, especially Cu/engine oil nanofluids, compared to conventional base fluids with other nanoparticles. It was noticed that the Nusselt number increases with decreasing nanoparticle diameter and also with increasing Reynolds number.

Keywords: Double backward-facing step, nanofluid, nanoparticles, nanoparticles size, laminar flow, heat transfer.

How to cite this article:
Alriqeeq, A.K.; Jolgam, S.A. Simulation of laminar nanofluids flow over a heated double backward-facing step. Univ Zawia J Eng Sci Technol. 2024;2:81-97.

محاكاة تدفق السوائل النانوية الصفائحية على خطوة ساخنة مزدوجة مواجهة للخلف

علي خليفة عبدالله الرقيق[1] ، شعبان أحمد علي جلغام[2]

[1]قسم الهندسة الميكانيكية والصناعية، كلية الهندسة جامعة صبراتة، صبراتة، ليبيا.
[2]قسم الهندسة الميكانيكية والصناعية، كلية الهندسة جامعة الزاوية، الزاوية، ليبيا.

ملخـــــص البحـــــث

يركز هذا البحث على تحسين انتقال الحرارة عن طريق فصل التدفق على خطوة مزدوجة موجهة للخلف باستخدام السائل

النانوي. لإجراء هذا البحث، تم إنشاء نموذج عددي باستخدام ANSYS Workbench، وتم حل المعادلات الحاكمة باستخدام نموذج Realizable k-ε بدقة من الدرجة الثانية. تم استخدام ثلاثة أنواع مختلفة من السوائل الأساسية (الماء، زيت المحرك، جلايكول الإيثيلين) مع الجسيمات النانوية (Cu ،Tio_2 ،AL_2O_3) لأرقام رينولدز تتراوح من 200 إلى 1000. وتم تسليط فيض حراري ثابت $2000\ W/m^2$ على الجدار السفلي. تم دراسة تأثير تراكيز الجسيمات النانوية وأحجام الجسيمات النانوية وأرقام رينولدز على رقم نسلت. تم استخدام طريقتين مختلفتين لإيجاد الموصلية الحرارية واللزوجة للسوائل النانوية. تم التحقق من نتائج البرنامج باستخدام النتائج العددية المنشورة سابقًا. أظهرت النتائج أن ذروة رقم نسلت تحدث بعد الخطوات مباشرة. أظهرت النتائج تحسنا ملحوظا في أداء انتقال الحرارة للسوائل النانوية، وخاصة سوائل النحاس/زيت المحرك النانوية، مقارنة بالسوائل الأساسية التقليدية مع الجسيمات النانونية الأخرى. وقد لوحظ أن رقم نسلت يزداد مع انخفاض قطر الجسيمات النانوية وكذلك مع زيادة رقم رينولدز.

الكلمات المفتاحية: خطوة مزدوجة موجهة للخلف، السوائل النانوية، الجسيمات النانوية، حجم الجسيمات النانوية، التدفق الصفائحي، انتقال الحرارة.

1. Introduction

As the global need for energy is growing, the heat transfer rate is one of the most significant parameters for systems that produce this energy. Thus, for a long time, many researchers in this area have been working to improve the performance of systems in terms of heat transfer rate. Heat transfer techniques have been adopted and investigated to enhance heat transfer. Separation and reattachment are the most crucial methods, which can be induced by flow over a forward-facing step (FFS) or a backward-facing step (BFS). Despite the simple geometry of BFS, it leads to complicated fluid flow dynamics. For instance, the sudden expansion causes flow separation, creating a recirculation zone with vortices. This type of separated flow can reduce energy efficiency due to losses, but it can also enhance heat transfer as a result of increased turbulent mixing [1].

Another technique to enhance heat transfer is by altering the thermal properties of fluids using nanofluids. Nanofluids are suspensions having diameters of fewer than 100 nanometres, and the nanoparticle concentration usually varies from 1% to 10%. Four mechanisms primarily drive thermal conductivity enhancement in nanofluids: the Brownian motion of the nanoparticles, liquid layering, the nature of heat transport in the nanoparticles, and the effects of nanoparticle clustering [2]. The convection heat transfer was found to be increased compared to that of base fluids such as water, oil, and ethylene glycol. Many studies have shown that nanofluids have excellent thermophysical properties, which have been extensively studied but are still controversial. A novel strategy to enhance heat transfer performance for thermal systems is adding nano-sized particles to the base fluid.

The numerical investigation conducted by [3] was the first to examine the impact of nanofluid on fluid flow and heat transfer in a backward-facing stepped channel. In this study, nanoparticles such as Cu, Ag, CuO, Al_2O_3, and TiO_2 were dispersed in water, which served as the base fluid. The numerical results revealed an increase in the average Nusselt number, specifically for TiO_2 within the recirculation zones. Additionally, it was observed that nanoparticles with high thermal conductivity, such as Ag or Cu, had a more significant effect on the Nusselt number outside the recirculation zones. Tinney and Ukeiley in [4] performed an experimental study of flow over a three-dimensional double-backward-facing step. Their results showed the formation of a horseshoe vortex after each step.

Al-Aswadi et al. in [5] utilised numerical simulations to examine the impact of seven different nanofluids (Au, Ag, Al_2O_3, Cu, CuO, SiO_2, and diamond) as they flowed through a backward-facing step configuration. The researchers observed the formation of a recirculation region in the nanofluid after passing through the step. They also noted that the length of the reattachment point increased with higher Reynolds numbers. Furthermore, the nanofluid containing SiO_2 nanoparticles exhibited the highest velocity among the nanofluids investigated, while the nanofluid with Au nanoparticles displayed the lowest velocity.

Mohammed et al. in [6] numerically investigated the effect of different types of nanoparticles (Au, Ag, Al_2O_3, Cu, CuO, SiO_2, TiO_2, and diamond) and water as base fluid on the fluid flow and heat transfer over a backward-facing step channel. It was observed that a recirculation zone was present after the step for all nanofluids studied. The highest Nusselt number (Nu) downstream of the primary recirculation zone was recorded for SiO_2 nanofluid, whereas diamond nanofluid exhibited the highest Nusselt number within the primary recirculation zone. Moreover, the skin friction coefficient was found to decrease as the Reynolds number increased. Togun et al. have numerically studied flow and heat over a double backward-facing step with different step heights and Reynolds numbers ranging from 98.5 to 512. The simulations were performed using ANSYS ICEM for the meshing process and ANSYS Fluent 14 for solving the governing equations. The top of the wall and the bottom of the upstream were insulated, while the bottom of the downstream was heated with a constant heat flux ($q = 2000$ W/m^2). The authors observed the formation of a recirculation zone after the first and second steps, and the Nusselt number increased in this region with an increase in Reynolds number and a decrease in step height [7]. Also, Togun et al. in [8] investigated the effects of obstacles on heat transfer and laminar fluid flow over a backward-facing step. The Reynolds number varied from 75 to 225, and the findings indicate that the recirculation region and heat transfer coefficient are higher in backward-facing step flows with obstacles compared to those without obstacles.

Togun et al. in [9] conducted a numerical investigation on the forced convection heat transfer of Cu/water nanofluid. The nanofluid had volume fractions (φ) ranging from 0% to 4%. The study examined Reynolds numbers in the range of 50 to 200 for the laminar regime and 5000 to 20000 for the turbulent regime. The researchers performed their analysis in a backward-facing step configuration, utilising a constant heat flux of 4000 W/m^2 as a boundary condition. They employed the finite-volume method and utilised Fortran code to solve equations related to continuity, momentum, energy, and turbulence. The study revealed that the maximum Nusselt number occurred after the step, owing to the formation of a recirculation zone. As the Reynolds number increased, the Nusselt number also increased [9]. The laminar and turbulent regimes achieved maximum thermal efficiencies of approximately 26% and 36%, respectively. The effect of two types of nanoparticles, SiO_2 and Al_2O_3, and distilled water as the base fluid on fluid flow and heat transfer through a microscale backward-facing step channel was experimentally and numerically investigated by [10].

The nanoparticle volume fraction in the base fluid varied from 0 to 0.01. The study's results indicated that the Nusselt number (Nu) increased with increasing volume fractions of nanoparticles. The researchers also found that the SiO_2/water nanofluid had the highest Nusselt number and a lower friction factor compared to the Al_2O_3/water nanofluid. A study was conducted by [11] to examine the thermal-hydraulic properties of a mixture of Al_2O_3 and water nanofluid with volume fractions (φ) ranging from 1% to 5%. The focus was on a single backward-facing step with an expansion ratio of 2, and the Reynolds numbers (Re) ranged from 100 to 500. The results indicated that the local Nusselt number increased rapidly to its maximum value at the separation point and then gradually decreased along the heated wall until it reached a nearly constant shape.

Lv et al. in [12] studied the turbulent flow characteristics of SiO_2/water nanofluids through a backward-facing step (BFS) using particle image velocimetry (PIV). They found the number of vortexes and the turbulent kinetic energy increased when the volume concentration of nanofluids increased at the same Reynolds number (Re). At a 3% volume fraction of nanoparticles in the nanofluid and a Reynolds number of 5000, the number of vortices, turbulent kinetic energy, and average vorticity increase by three times, 368%, and 22.1%, respectively, as compared to the fluid being pure water. In their contribution, Abdulrazzaq et al. in [13] numerically investigated the convection flow of different convectional fluids (water, ammonia liquid, and ethylene glycol) through a double backward-facing step channel with different step heights and Reynolds numbers in the laminar region from 98.5 to 512. The study examined a constant heat flux (q = 2000 W/m^2) at the downstream wall. The obtained results indicated that the Nusselt number (Nu) increases after the recirculation region at the first and second steps with an increase in Reynolds number (Re). Ethylene glycol presented the highest heat transfer performance among the other working fluids. In a recent study by [14], three non-rotating adiabatic cylinders were employed in the backward-facing step configuration to enhance heat transfer. The investigation included Reynolds numbers ranging from 50 to 250, and three different heat fluxes (q = 250, 500, and 750 W/m^2) were applied as boundary conditions on the lower wall of the channel. The findings demonstrated that the incorporation of cylinders led to a reduction in the reattachment length and an improvement in heat transfer efficiency by 6% to 13%.

This paper investigates the effect of adding nanoparticles to other base fluids, namely, engine oil and ethylene glycol, on the flow characteristics over a heated double backward-facing step. It also presents the assessment of two different approaches used in the previous literature to estimate the properties of nanofluids utilised in obtaining the Nusselt number.

2. Computational Model

Two models have been created by using ANSYS, which are the periodic domain to get the fully developed flow and the main domain for simulating the separation of flow and heat transfer through a double backward-facing step.

2.1 Periodic Domain

A periodic domain is constructed as shown in Figure 1. It is a small portion of a channel with a length (L = 10 mm) and height (H = 4.8 mm). It is used to obtain fully developed flow at the inlet of the channel, in order to skip the stage of the entrance length in the simulation process.

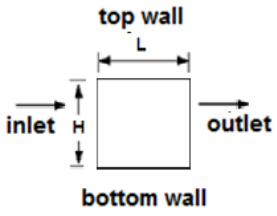

Figure 1: Schematic diagram of the periodic domain

2.2 Main Domain

This study is based on the previous work of [1] who have used the dimensions presented in Figure 2.

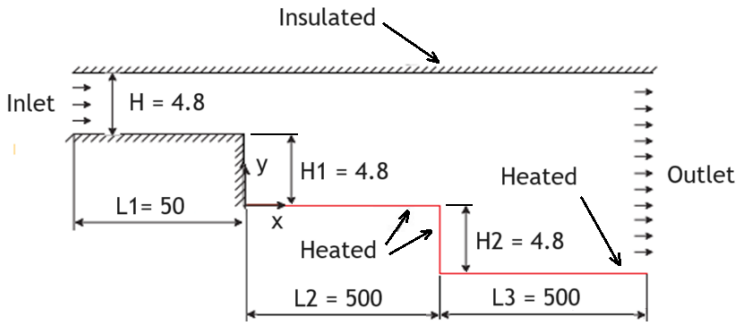

Figure 2: Schematic diagram of the main domain, all dimensions are in mm.

2.3 Methodology

In this study, a computational investigation of nanofluid flows through a heated double backward-facing step channel is carried out using ANSYS Fluent software. Nanoparticles of Cu, Al_2O_3 and TiO_2 with base fluids of water, engine oil and ethylene glycol are used. Laminar fluid flows with Reynolds numbers of 200, 400, 600, 800, and 1000 are employed. The study includes the investigation of the effect of (i) Reynolds numbers, (ii) nanoparticle material, (iii) nanoparticle concentration and (iv) nanoparticle diameter on the Nusselt number.

2.4 Governing Equations

In the used two-dimensional model, the nanofluids are handled as Newtonian, steady, and single-phase incompressible fluids. The conservation equations based on the Navier-Stokes equations for a single-phase fluid are used to describe the nanofluid flow over a double backward-facing step. These equations are continuity, momentum, and energy, which are written based on the above-mentioned assumptions as follows:

$$\frac{\partial u}{\partial x}+\frac{\partial v}{\partial y}=0 \tag{1}$$

$$u\frac{\partial u}{\partial x}+v\frac{\partial u}{\partial y}=-\frac{1}{\rho}\frac{\partial p}{\partial x}+\nu\left(\frac{\partial^2 u}{\partial x^2}+\frac{\partial^2 u}{\partial y^2}\right) \tag{2}$$

$$u\frac{\partial v}{\partial x}+v\frac{\partial v}{\partial y}=-\frac{1}{\rho}\frac{\partial p}{\partial y}+\nu\left(\frac{\partial^2 v}{\partial x^2}+\frac{\partial^2 v}{\partial y^2}\right) \tag{3}$$

$$u\frac{\partial T}{\partial x}+v\frac{\partial T}{\partial y}=-\frac{1}{\rho}\frac{\partial p}{\partial y}+\alpha\left(\frac{\partial^2 T}{\partial x^2}+\frac{\partial^2 T}{\partial y^2}\right) \tag{4}$$

where u is the x-component of velocity, v is the y-component of velocity, ρ is the density, ν is the kinematic viscosity, α is the thermal diffusivity and T is the temperature. The Reynolds number is defined as follows:

$$Re=\frac{\rho v L_h}{\mu} \tag{5}$$

where L_h is the hydraulic (characteristic) length. The local convective heat transfer coefficient h_x on the wall is given by:

$$h_x=\frac{q_w}{T_w-T_b} \tag{6}$$

where q_w is the wall heat flux, T_w is wall temperature, and T_b is the bulk flow temperature. The average Nusselt number Nu_{avg} can be obtained as follows:

$$Nu_{\mathrm{avg}} = \frac{D}{k}\int_0^L h_x dx \tag{7}$$

The modelled transport equations for k and ε in the realizable k- ε model are given as follows [15]**:**

$$\frac{\partial}{\partial \mathrm{t}}(\rho \mathrm{k}) + \frac{\partial}{\partial \mathrm{x_j}}\left(\rho \mathrm{k u_j}\right) = \frac{\partial}{\partial \mathrm{x_j}}\left[\left(\mu + \frac{\mu_t}{\sigma_\varepsilon}\right)\frac{\partial \mathrm{k}}{\partial \mathrm{x_j}}\right] + \mathrm{G_k} + \mathrm{G_b} - \rho\varepsilon - \mathrm{Y_M} + \mathrm{S_k} \tag{8}$$

and

$$\frac{\partial}{\partial \mathrm{t}}(\mathrm{p}\varepsilon) + \frac{\partial}{\partial \mathrm{x_j}}\left(\rho \mathrm{k}\varepsilon \mathrm{u_j}\right) = \frac{\partial}{\partial \mathrm{x_j}}\left[\left(\mu + \frac{\mu_t}{\sigma_\varepsilon}\right)\frac{\partial \varepsilon}{\partial \mathrm{x_j}}\right] + \rho \mathrm{C_1 S}\varepsilon + \rho \mathrm{C_2}\frac{\epsilon^2}{\mathrm{k} + \sqrt{\mathrm{v}\varepsilon}} + \mathrm{C_{1\varepsilon}}\frac{\varepsilon}{\mathrm{k}}\mathrm{C_{3\varepsilon}G_b} + \mathrm{S_\varepsilon} \tag{9}$$

where,

$$C_1 = \max\left[0.43, \frac{\eta}{\eta + 5}\right], \qquad \eta = S\frac{\mathrm{k}}{\varepsilon} \qquad S = \sqrt{2S_{ij}S_{ij}}$$

In these equations, G_K represents the generation of turbulence kinetic energy due to mean velocity gradients, G_b is the generation of turbulent kinetic energy due to buoyancy, and Y_M is the contribution of the fluctuating dilatation in compressible turbulence to the overall dissipation rate. G_2 and $C_{1\varepsilon}$ are constants. σ_k and σ_ε are the turbulent Prandtl numbers for k and ε, respectively. S_k and S_ε are user defined source terms. The model for turbulent eddy viscosity is presented in the following form:

$$\mu_t = \rho C_\mu \frac{k^2}{\varepsilon} \tag{10}$$

The C_μ in the realizable $k - \varepsilon$ model is not constant and calculated as follows:

$$C_\mu = \frac{1}{A_0 + A_S\frac{KU^*}{\varepsilon}} \tag{11}$$

where,

$$U^* = \sqrt{S_{ij}S_{ij} + \widetilde{\Omega}_{ij}\widetilde{\Omega}_{ij}} \tag{12}$$

and,

$$\widetilde{\Omega}_{ij} = \Omega_{ij} = 2\varepsilon_{ijk}\omega_k \tag{13}$$

$$\Omega_{ij} = \overline{\Omega}_{ij} = 2\varepsilon_{ijk}\omega_k \tag{14}$$

where $\overline{\Omega}_{ij}$ is the mean rate-of-rotation tensor viewed on a moving reference frame with an angular velocity ωk. The model constants A_0 and A_s are given by:

$$A_0 = 4.04, \quad A_s = \sqrt{6}\,cos\emptyset \tag{15}$$

where,

$$\emptyset = \frac{1}{3}cos^{-1}\left(\sqrt{6}W\right), \qquad W = S_{ij}S_{ik}S_{ki}, \qquad \tilde{S} = \sqrt{S_{ij}S_{ij}}, \qquad S_{ij} = \frac{1}{2}\left(\frac{\partial \mu_j}{\partial x_i} + \frac{\partial \mu_i}{\partial x_j}\right)$$

and the constant variables of the model are as follows:

$C_{1\varepsilon}$= 1.44, C_2 = 1.9, σ_k = 1.0, σ_ε = 1.2

2.5 Nanofluid Properties

The three main properties involved in calculating the heat transfer rate of the nanofluids are their heat capacity, viscosity, and thermal conductivity, which are quite different from those of the base fluids. The thermophysical properties in the governing equations are replaced by the properties of the nanofluids.

Nanofluid density (ρ_{nf}) is estimated by measuring the volume and weight of the liquid and particle densities $\rho_f$and ρ_{np}, respectively, using the model given in [16] as follows:

$$\rho_{nf} = (1-\varphi)\rho_f + \varphi\rho_{np} \tag{16}$$

where φ is the volume fraction, and the subscripts *nf*, *f*, and *np*, denote the nanofluid, base fluid and nanoparticle, respectively. Assuming thermal equilibrium between the nanoparticles and the base fluid, the specific heat of the nanofluids (C_{pnf}) can be obtained by using the relation presented in [17]:

$$C_{pnf} = \frac{(1-\varphi)(\rho C_p)_f + \varphi(\rho C_p)_{np}}{\rho_{nf}} \tag{20}$$

where C_p is the heat capacity.

There are two different approaches used to estimate the thermal conductivity (k_{nf}) and viscosity (μ_{nf}) of the nanofluids; the first approach does not consider the nanoparticle size in estimating thermal conductivity and viscosity, which are given in [18] and [19], respectively, as follows:

$$k_{nf} = k_f \frac{k_{np} + 2k_f + 2\varphi(k_{np} - k_f)}{k_{np} + 2k_f - \varphi(k_{np} - k_f)} \tag{21}$$

The viscosity of the nanofluids (μ_{nf}) has been determined as follows:

$$\mu_{nf} = \mu_f(1 + 5\varphi + 80\varphi^2 + 160\varphi^3) \tag{22}$$

The thermophysical properties of base fluids and nanoparticles at 300 K are listed in Table 1.

Table 1: Thermophysical properties of base fluids and nanoparticles at 300 K.

Materials	P [kg/m^3]	C_p [J/kg K]	k [W/m^2 K]	M [kg/m s]
Water (H_2O)	997.1	4170	0.6	0.001
Ethylene glycol (EG)	1114.4	2415	0.252	0.0157
Engine oil (EO)	889	1845	0.145	1.06
Copper (Cu)	8933	385	400	-
Alumina (Al_2O_3)	3970	765	40	-
Titania (TiO_2)	4250	686.2	8.953	-

On the other hand, the second approach is based on nanoparticle size in estimating the properties of nanofluids; the empirical correlation given in [20] is used to calculate the effective thermal conductivity (k_{eff}). This model incorporates the Brownian motion in nanoparticles into Maxwell's theory.

$$k_{\text{eff}} = k_{\text{static}} + k_{\text{Brownian}} \tag{23}$$

$$k_{\text{static}} = k_f \left[\frac{k_{np} + 2k_f + 2\varphi k_f (k_{np} - k_f)}{k_{np} + 2k_f - \varphi k_f (k_{np} - k_f)} \right] \tag{24}$$

$$k_{\text{Brownian}} = 5 \times 10^4 \beta \varphi \rho_f C_{p,f} \sqrt{\frac{KT}{2\rho_{np}\, d_p}} f(T, \varphi) \tag{25}$$

Where K = 1.3809× 10^{-23}J/K is the Boltzmann constant, T is the temperature (K) and β is given as:

$$\beta = 8.4407(100\varphi)^{-1.07304}$$

and $f(T, \varphi)$ is given as:

$$f(T, \varphi) = (2.8217 \times 10^{-2}\varphi + 3.917 \times 10^{-3})$$

Equations developed by [21] were used to calculate the effective dynamic viscosity (μ_{eff}) of the nanofluid:

$$\mu_{\text{eff}} = \mu_f \frac{1}{(1 - 34.87(d_p/d_f)^{-0.3} \times \varphi^{1.03})} \tag{26}$$

where d_p represents the mean diameter of the nanoparticles, d_f the equivalent diameter of a base fluid molecule:

$$d_f = \left(\frac{6M}{N\pi\rho_{f0}} \right)^{1/3} \tag{27}$$

where M is the molecular weight, and N is the Avogadro number (6.022 × 10^{23} mol^{-1}), and ρ_{f0} is the density of the base fluid found at temperature = 293 K.

2.6 Mesh Generation

A structured uniform grid has been generated using the meshing tool in ANSYS FLUENT. Where the number of cells or the element size can be specified. Edge sizing was used, the size of the mesh for the periodic domain is chosen to be 20 × 10 as shown in Figure 3. A face meshing with 2D structured quadratic elements of 0.5 mm size is set to the main domain as illustrated in Figure 4. The mesh total elements and nodes are 51000 and 53131, respectively.

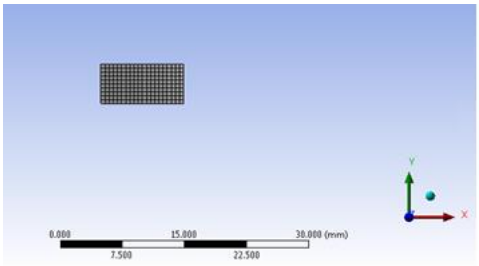

Figure 3: Mesh structure used for periodic domain

2.7 Boundary Conditions for Periodic Domain

Boundary conditions for the periodic domain are stationary wall, no-slip, planar, constant heat flux (zero). For the periodic domain either the mass flow rate or pressure gradient (Pa/m) is needed to be given as input for the periodic conditions. In order to calculate the pressure gradient, which is used in

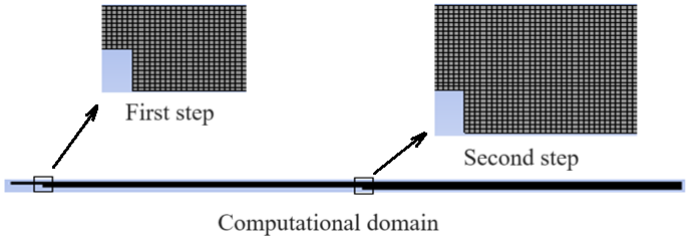

Figure 4: Structured mesh for main domain, (a) First step region and (b) Second step region.

this study. A Reynolds number of 200 is used in the sample of calculations to calculate the flow velocity. The hydraulic (characteristic) length is calculated as follows:

$$L_h = \frac{2ab}{a+b} \tag{28}$$

where a = 0.0048 m and b = 1 m are the height and width of the channel, respectively. Substituting these values in the above equation (28) yields:

$$L_h = \frac{2 \times 0.0048 \times 1}{0.0048 + 1} = 0.00955 \text{ m}$$

The viscosity of the nanofluid can be calculated using equation (22):

$$\mu_{nf} = 0.001(1 + 5 \times 0.03 + 80 \times 0.03^2 + 160 \times 0.03^3) = 0.00122 \text{ kg/ms}$$

The density of the nanofluid can be calculated using equation (16):

$$\rho_{nf} = (1 - 0.03)997.1 + 0.03 \times 8933 = 1235.17 \text{ Kg/m}^{-3}$$

The flow inlet velocity can be calculated from Reynolds number, equation (5), as follows:

$$v = \frac{0.00122 \times 200}{1235.17 \times 0.00955} = 0.02068$$

The pressure gradient is calculated using the following equation:

$$\Delta P = f \frac{L}{D} \frac{\rho v^2}{2} \tag{29}$$

For rectangular cross-section $b/a \approx \infty$, the friction factor f for laminar flow is calculated using the following equation [22]:

$$f = \frac{96}{Re} = \frac{96}{200} = 0.48 \tag{30}$$

$$\Delta P = 0.48 \frac{1}{0.00955} \frac{1235.17 \times 0.02068^2}{2} = 13.275 \frac{\text{Pa}}{\text{m}}$$

2.8 Boundary Conditions for Main Domain

Boundary conditions for the main domain are walls with no slip, inlet in which the velocity magnitude set as periodic axial velocity (to be read from output data file obtained from periodic domain) instead of constant, and pressure outlet condition is enforced at the outlet boundary. On the upstream and first step walls, an adiabatic wall boundary condition is enforced on the downstream walls a constant heat

flux is applied. Figure 5 shows the boundary conditions applied to the main geometry. The detailed values of these conditions are presented in Table 2.

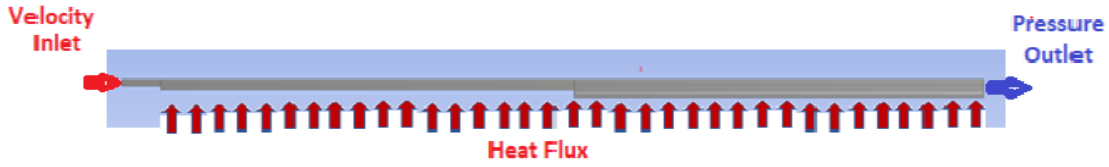

Figure 5: Boundary conditions for main geometry

Table 2: Boundary conditions.

Boundary	Boundary conditions
Inlet	Inlet velocity
Outlet	Standard pressure
Upstream first step and upper wall	Insulated
Downstream first step walls	Heat flux = 2000 W/m2

2.9 Numerical Settings

When conducting simulations with CFD software, the user must choose the appropriate models to solve the problem. As it was decided to use the homogenous (single-phase) model, the multiphase model was not activated for this study. The realizable k-ε turbulence model with enhanced wall treatment was chosen as the viscous model for this study. In addition to the model selection, different solvers were also tested. With this investigation, the aim was to find a solver that resulted from which the solution converged. In all cases, the coupled solver was chosen, as it is the most effective solution for the pressure and the velocity components. The second-order upwind scheme was used to solve momentum and energy equations as it offers a good balance between accuracy and stability for solving partial differential equations and to capture the correct flow behaviour. Once the numerical model has been set up, and convergence criteria are set up. The convergence criteria of various parameters (continuity, x-velocity, y-velocity, energy, k, and ε) are taken as 10^{-6}. The solution was initialized using the standard initialization method.

3. Results and Discussion

This section focuses on the presentation and discussion of the results gained from the simulations conducted. Results include verification of the results and studying the effect of varying steps height, the effect of using nanofluids over normal fluids, and the effect of base fluid, nanoparticle type, and nanoparticle concentration, on both heat performance and hydraulic performance.

3.1 Mesh dependence study

The relationship between shear stress and grid intensity is presented in Figure 6 for six distinct meshes at a Reynolds number of Re = 200 using 3% Cu/water nanofluid. It can be noticed that the fifth mesh provides an acceptable approximate solution, as further refinement of the mesh beyond this point does not significantly influence the estimated solution.

3.2 Verification of the Results

As mentioned earlier the simulations were carried out using the k-ε model with the near wall function for the resolution of the viscous sublayer of the boundary layer. The results of the

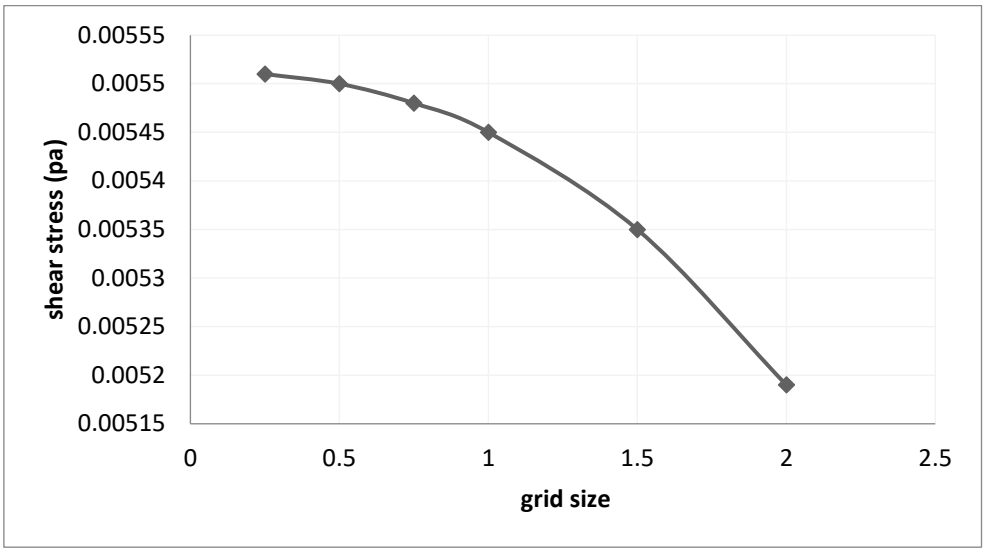

Figure 6: Grid independence study

wall y+ value in the axial direction is shown in Figure 7. It can be seen that the dimensionless distance y+ is less than 5, which means that the grid is refined enough in the near-wall region. In order to verify the present CFD simulations, the current results are compared with the available numerical results in the literature.

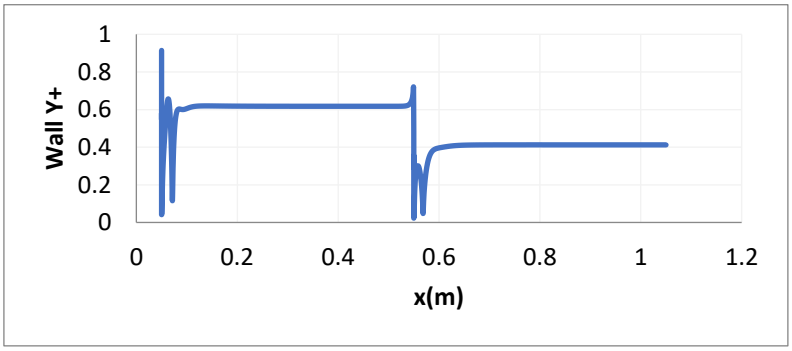

Figure 7: The wall y+ value at the wall along the axial direction

Figure 8 shows the comparison between the current computed results of the local heat transfer coefficient along the axial direction with the numerical results of [7] for a single backward step with Re = 75. The current computed results agree reasonably well with the reference results.

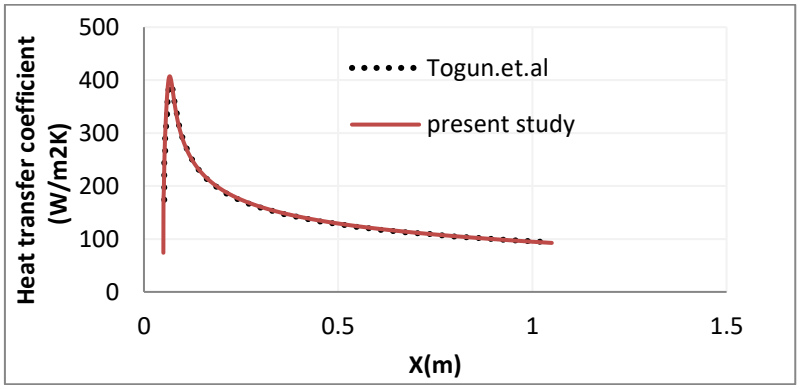

Figure 8: Comparison of the current numerical results of the heat transfer coefficient with those of [7].

3.3 Effect of Reynolds Number on Nusselt Number

It is commonly known that heat transfer increases with increasing Reynolds number. The results of this study are displayed in terms of the Nusselt number. The effect of the Reynolds number on the Nusselt number along the channel for 3% Cu/water nanofluids is shown in Figure 9. The Nusselt number increases with an increase in the Reynolds number. This is due to the enhancement in heat transfer at a higher Reynolds number and due to an increase in Brownian motion for the nanofluids at higher Reynolds numbers. The Brownian motion arises due to the collision of the particles with the fluid molecules. These collisions cause the particles to change direction and speed in a random manner. Notice that the value Nusselt number increases after the first and second steps due to flow separation caused by sudden expansion, and this leads to the destruct of the thermal boundary layer and forming a recirculation zone consisting of vortices. The size of the vortices increases by increasing the Reynolds number.

3.4 Effect of Nanoparticle Material on Nusselt Number

In order to study the effect of nanoparticle materials on the heat transfer in nanofluids, each of the nanoparticles is compared to another with water at 9% concentration. Figure 10 presents comparisons of the local Nusselt Number for pure water, Cu/water, Al_2O_3/water, and TiO_2/water. The results show that the heat transfer enhancement increases with the presence of nanoparticles and increases with nanoparticle thermal conductivity.

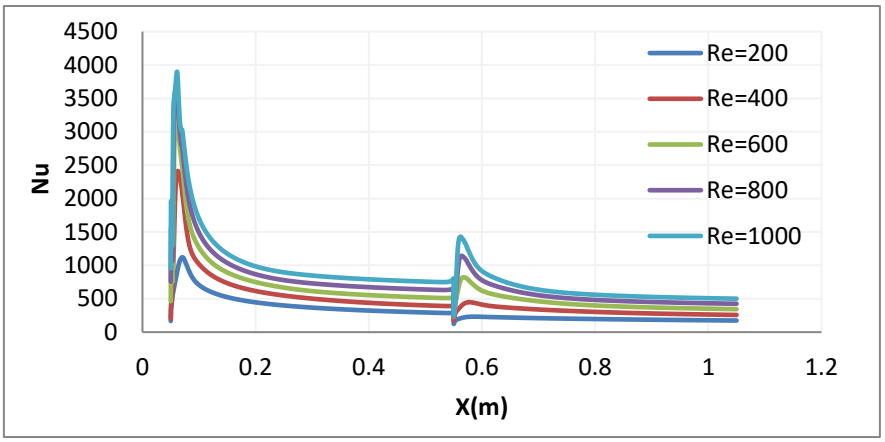

Figure 9: Variations of local Nusselt number along the channel for different Reynolds numbers for 3% Cu/water nanofluids.

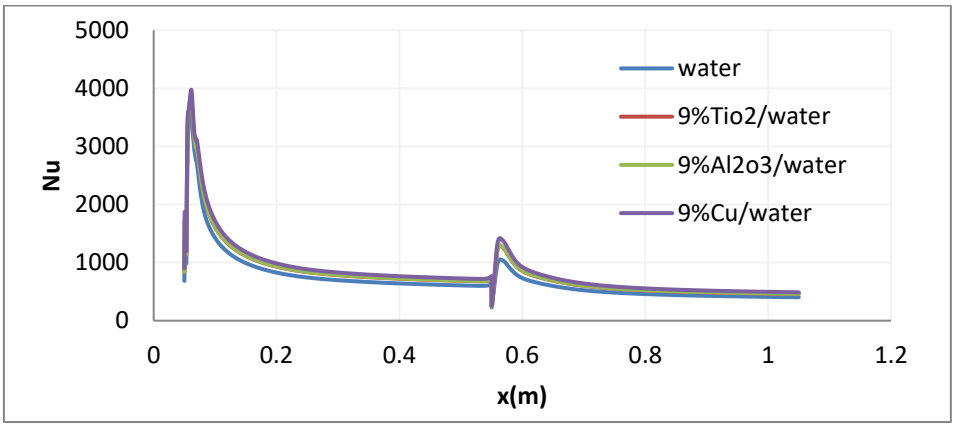

Figure 10. Local Nusselt Number coefficient at Re = 800 for water nanofluids with different nanoparticle materials

Figure 11 shows the average Nusselt number against Re for different nanoparticle materials. The results show that the Nusselt Number of the Cu/water nanofluid is higher than that of other nanofluids. This is due to the higher thermal conductivity of Cu particles. The highest enhancement was achieved by Cu/water nanofluids with a 981.301 Nusselt number as compared to pure water's 820.126 at Re = 1000. This was followed by AL_2O_3/water nanofluids and TiO_2/water with 927.390 and 923.154, respectively.

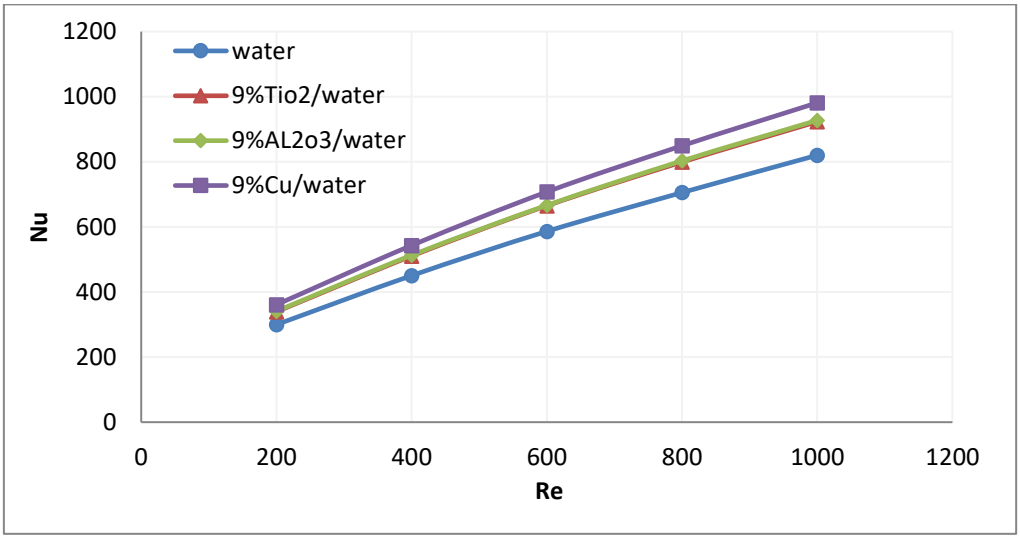

Figure 11. Average Nusselt number for water nanofluids with different nanoparticle materials

3.5 Effect of Nanoparticle Concentration on Nusselt Number

To investigate the effect of the nanoparticle concentration on the heat transfer in nanofluids, the concentration of Cu/water nanofluid. For comparison, pure water, 3% Cu/water, 6% Cu/water, and 9% Cu/water nanofluids are investigated for the wall along the axial direction. In Figure 12 at Re = 800, it can be seen that the Nusselt number increases with the increase in nanoparticle volume concentration. This is due to the improved convective heat transfer performance with the increased nanoparticle concentration.

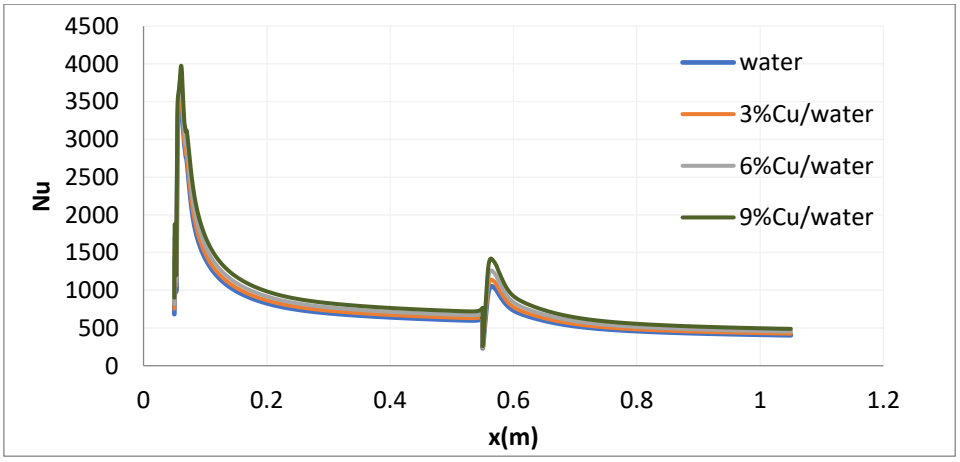

Figure 12: Nusselt number at Re = 800 for different concentrations of Cu/water nanofluid.

For different fractions of nanofluid particles of Cu nanofluid in water, Figure 13 shows the average Nusselt number against Re. The results show that the addition of nanoparticles can increase the heat transfer substantially compared to water alone. It was observed that the heat transfer rate enhanced as the particle volume fraction increased at any given Reynolds number. This enhancement increases as the Reynolds number increases. The obtained average Nusselt number at a Reynolds number of 1000 for 9% Cu/water, 6% Cu/water, 3% Cu/water, and pure water is 981.30, 908.67, 855.9 and 820.12, respectively. It can be noticed that the maximum value of the average Nusselt number is obtained using 9% Cu/Water.

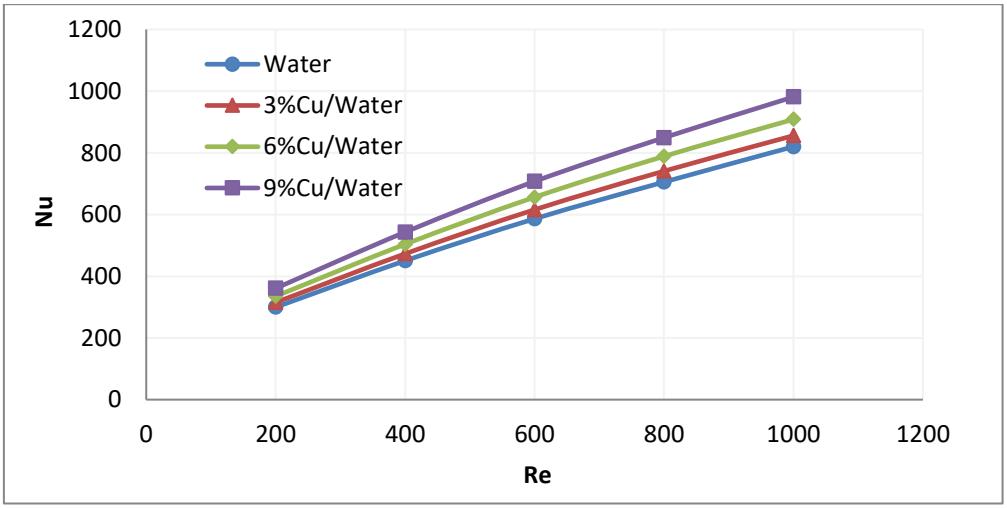

Figure 13: Average Nusselt Number versus Reynolds number for Cu/Water nanofluids.

3.6 Effect of Base Fluids on Nusselt Number

In order to examine how the type of base fluid affects the performance of nanofluids, it is important to first analyse the individual performance of each fluid. Figure 14 displays the average Nusselt number for each base fluid without the presence of nanoparticles. One can notice that the engine oil and ethylene glycol exhibit superior performance compared to water, which can be attributed to the

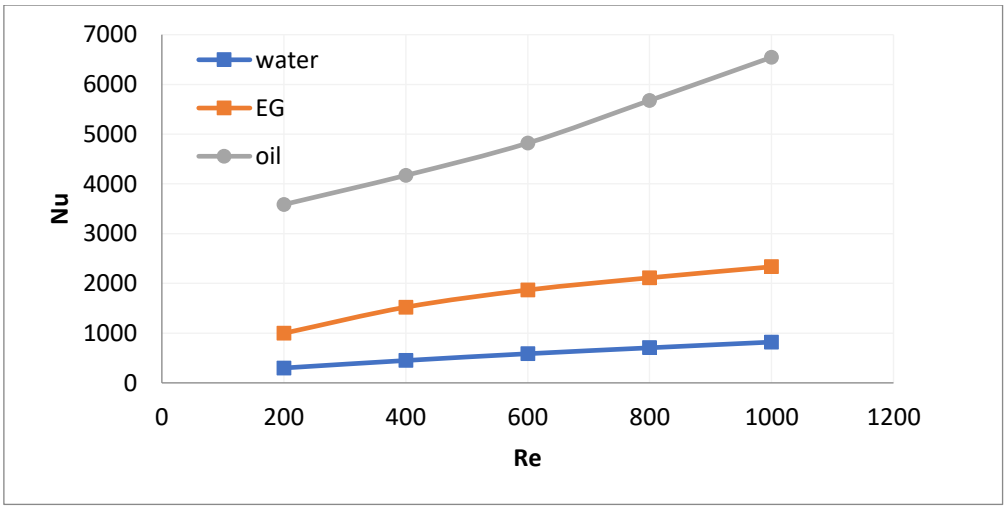

Figure 14: Average Nusselt number versus Reynolds number for different base fluids.

difference in properties of each base fluid. This is because engine oil and ethylene glycol have higher thermal conductivities and specific heat capacities compared to water. This means that they are better at conducting heat and can absorb more heat energy per unit mass, resulting in higher heat transfer rates. Additionally, they have higher viscosities than water, which increases flow resistance and enhances convective heat transfer. These properties collectively contribute to the higher performance of engine oil and ethylene glycol as base fluids in heat transfer applications.

Incorporating nanoparticles into a base fluid can significantly enhance its heat transfer capabilities compared to the fluid without nanoparticles. Figure 15 displays the average Nusselt number for various base fluids with a 9% volume concentration of Cu nanoparticles. The outcomes reveal that water exhibits the least improvement in heat transfer, despite having the highest thermal conductivity as given in Table 1. This can be attributed to the higher Prandtl number of engine oil and ethylene glycol in comparison to water, which affects the convective heat transfer performance.

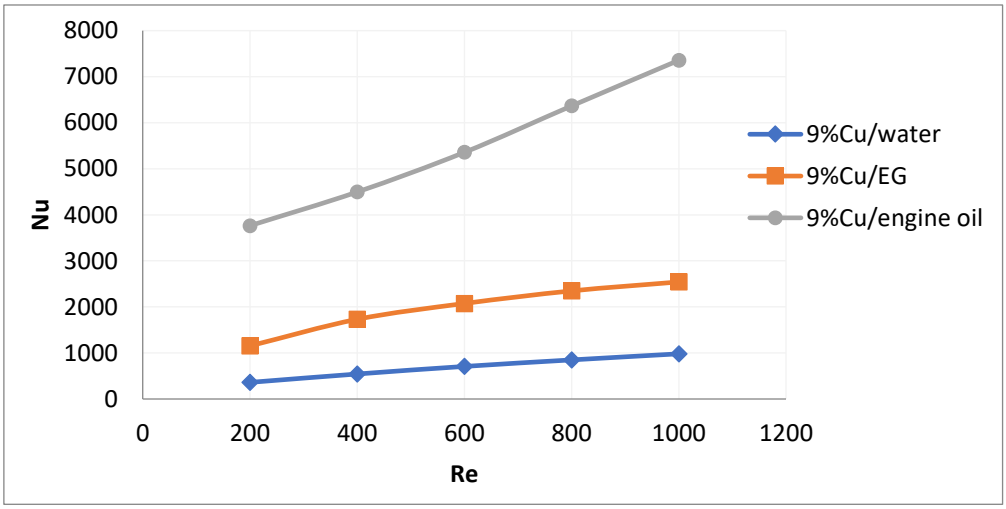

Figure 15: Average Nusselt number versus Reynolds number for 9% Cu particles with different base fluids.

3.7 Effect of Nanoparticle Diameter

Nanoparticle size impacts the Nusselt number values when the set of equations (23-26) are used as shown Figure 16, these equations consider the particle diameter (dp), which significantly influences the calculation of dynamic viscosity and thermal conductivity. The results are shown using 3% Cu/water nanoparticle diameter values, with a Reynolds number of 800. The values of the average Nusselt numbers are presented in Table 3. It is observed that the Nusselt number increases as the nanoparticle diameter decreases from 40 to 10 nm. This is attributed to the enhanced nanofluid viscosity associated with smaller diameters, along with the influence of Brownian motion, which promotes heat transfer augmentation. Furthermore, nanoparticles with smaller diameters will be more in number in comparison with nanoparticles with larger diameter. This, in turn, augments thermal conductivity, and viscosity.

Table 3: Average Nusselt number values obtained from set of equations (23-26).

Particle diameter, dp [nm]	Nusselt number, Nu
10	733.818
20	727.133
30	723.976
40	721.977

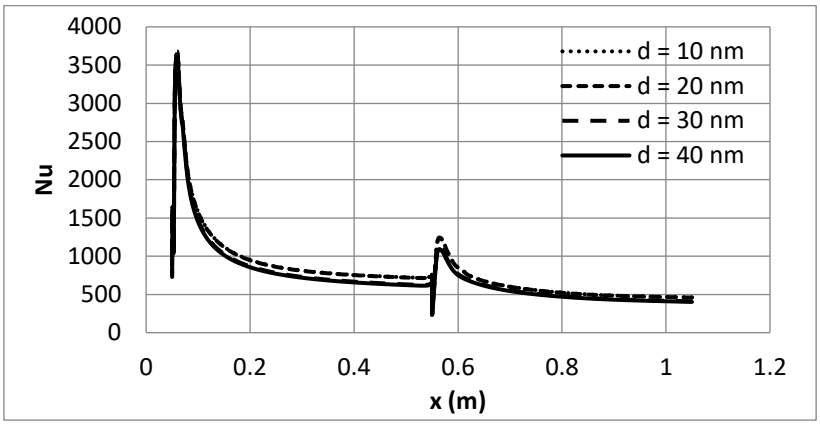

Figure 16: Local Nusselt number at Re = 800 for 3% Cu/water nanofluids at different diameters.

On the other hand, when using the set of equations (21, 22) solely considers the impacts of volume concentration (φ), which crucially affects the calculation of dynamic viscosity and thermal conductivity, resulting in an average Nusselt number of 740.902. Figure 17 shows the percentage decrease in average Nusselt number when the set of equations (23-26) are used.

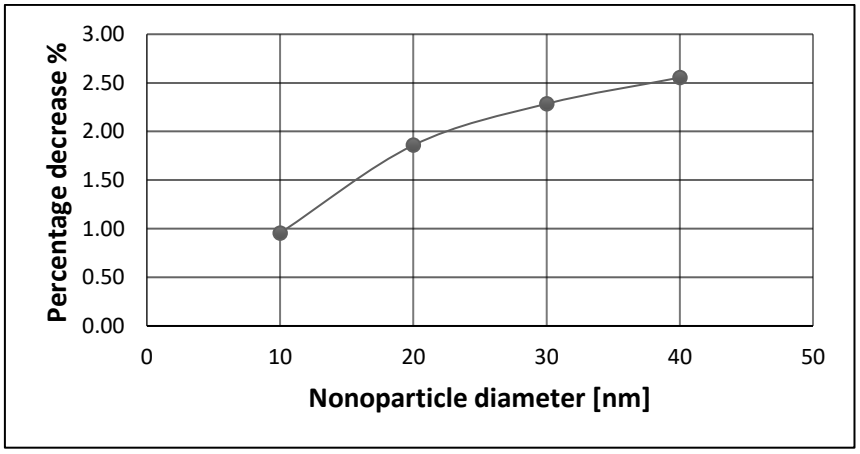

Figure 17: Percentage decrease in Nu values when using set of equations (23-26) compared to that obtained using set of equations (21, 22).

4. Conclusions

This paper thoroughly investigated the improvements in heat transfer of nanofluid laminar flow over a double backward-facing step under constant heat flux boundary conditions. Due to the turbulence that occurs after each step, the simulations were carried out using the realizable *k*-ε model. It is concluded that increasing the Reynolds number increases the Nusselt number. Using nanofluids enhances the heat transfer process under laminar flow conditions. The Cu nanoparticles enhance heat transfer more than other studied nanoparticles, i.e., Al_2O_3 and TiO_2. As the nanoparticle concentration increases, the Nusselt number increases. Nanofluids showed better heat transfer properties than base fluid alone. The best enhancement is obtained when engine oil base fluid is used, followed by ethylene glycol, then water. The Nusselt number increases as the diameter of nanoparticles decreases. The set of equations that consider nanoparticle size in estimating the nanofluid thermal conductivity and viscosity give a decrease in Nusselt number in the range of 0.96%–2.55% for nanoparticle diameters ranging from 10 nm to 40 nm over those obtained from the set of equations that do not.

REFERENCES

[1] Rana, S., Dura, H. B., Bhattrai, S., and Shrestha, R. (2021). Comparative Study of Thermal Performance of Different Nanofluids in a Double Backward-Facing Step Channel: A Numerical Approach. *International Journal of Chemical Engineerin*g, 2021, 1-14.

[2] Wang, X.-Q. and Mujumdar, A. S. (2008). A review on nanofluids-part i: theoretical and numerical investigations. *Brazilian journal of chemical engineering*, 25:613– 630.

[3] Abu-Nada, E. (2008). Application of nanofluids for heat transfer enhancement of separated flows encountered in a backward facing step. *International Journal of Heat and Fluid Flow*, 29(1):242–249.

[4] Tinney, C. and Ukeiley, L. (2009). A study of a 3-d double backward-facing step. *Experiments in Fluids*, 47:427–438.

[5] Al-Aswadi, A., Mohammed, H., Shuaib, N., and Campo, A. (2010). Laminar forced convection flow over a backward facing step using nanofluids. *International Communications in Heat and Mass Transfer*, 37(8):950–957.

[6] Mohammed, H., Al-aswadi, A., Abu-Mulaweh, H., and Shuaib, N. (2011). Influence of nanofluids on mixed convective heat transfer over a horizontal backward-facing step. *Heat Transfer—Asian Research*, 40(4):287–307.

[7] Togun, H., Abdulrazzaq, T., Kazi, S., Badarudin, A., and Ariffin, M. (2013). Heat transfer to laminar flow over a double backward-facing step. *Int. J. Mech. Ind. Sci. Eng*, 7:673–678.

[8] Togun, H., Abdulrazzaq, T., Kazi, S., Badarudin, A., Ariffin, M., and Zubir, M. (2014a). Numerical study of heat transfer and laminar flow over a backward facing step with and without obstacle. International Journal of Mechanical, Aerospace, *Industrial and Mechatronics Engineering*, 8(2):2.

[9] Togun, H., Safaei, M. R., Sadri, R., Kazi, S. N., Badarudin, A., Hooman, K., and Sadeghinezhad, E. (2014b). Numerical simulation of laminar to turbulent nanofluid flow and heat transfer over a backward-facing step. *Applied Mathematics and Computation*, 239:153–170.

[10] Kherbeet, A. S., Mohammed, H., Munisamy, K., and Salman, B. (2014). The effect of step height of microscale backward-facing step on mixed convection nanofluid flow and heat transfer characteristics. *International Journal of Heat and Mass Transfer*, 68:554–566.

[11] Ekiciler, R. (2019). A cfd investigation of al2o3/water flow in a duct having backward-facing step. *Journal of Thermal Engineering*, 5(1):31–41.

[12] Lv, J., Hu, C., Bai, M., Li, L., Shi, L., and Gao, D. (2019). Visualization of sio2-water nanofluid flow characteristics in backward-facing step using piv. *Experimental Thermal and Fluid Science*, 101:151–159.

[13] Abdulrazzaq, T., Togun, H., Alsulami, H., Goodarzi, M., and Safaei, M. R. (2020). Heat transfer improvement in a double backward-facing expanding channel using different working fluids. *Symmetry*, 12(7):1088.

[14] Tahseen, T. A., Eleiwi, M. A., and Hameed, A. F. (2020). Numerical study of fluid flow and heat transfer in a backward facing step with three adiabatic circular cylinder. J*ournal of Advanced Research in Fluid Mechanics and Thermal Sciences*, 72(1):80–93.

[15] ANSYS FLUENT THEORY GUIDE. Release (2015). Ansys Inc. USA, pp:51–54.

[16] Pak, B. C. and Cho, Y. I. (1998). Hydrodynamic and heat transfer study of dispersed fluids with submicron metallic oxide particles. *Experimental Heat Transfer an International Journal*, 11(2): 151–170.

[17] Xuan, Y. and Roetzel, W. (2000). Conceptions for heat transfer correlation of nanofluids. *International Journal of heat and Mass transfer*, 43(19):3701–3707.

[18] Maxwell, J. C. (1873). A treatise on electricity and magnetism, volume 1. Clarendon press.

[19] Etaig, S., Hasan, R., and Perera, N. (2016). Investigation of a new effective viscosity model for nanofluids. *Procedia Engineering*, 157:404–413.

[20] Koo, J. and Kleinstreuer, C. (2005). Impact analysis of nanoparticle motion mechanisms on the thermal conductivity of nanofluids. *International communications in heat and mass transfer*, 32(9):1111–1118.

[21] Corcione, M. (2010). Heat transfer features of buoyancy-driven nanofluids inside rectangular enclosures differentially heated at the sidewalls. *International Journal of Thermal Sciences*, 49(9):1536–1546.

[22] Çengel, Y. A. and Ghajar, A. J. (2020). HEAT AND MASS TRANSFER: Fundamenta and Applications. McGraw-Hill Education.